© Universiti Tun Hussein Onn Malaysia Publisher's Office

IJIE

http://penerbit.uthm.edu.my/ojs/index.php/ijie
ISSN : 2229-838X e-ISSN : 2600-7916

The International Journal of Integrated Engineering

Surface Metrology for Process Diagnostic of Ultrasonic Vibration Assisted Grinding

Mohd Fauzi Ismail[1*], Rahim Jamian[2], Mohamad Irwan Yahaya[1], Hiromi Isobe[3]

[1]College of Engineering,
Universiti Teknologi MARA, 40450 Shah Alam, Selangor, MALAYSIA

[2]Faculty of Engineering Technology,
University Tun Hussien Onn, 84500 Bukit Pasir, Johor, MALAYSIA

[3]Department of Mechanical Engineering,
Nagaoka University of Technology, Niigata 940-2188, JAPAN

*Corresponding Author

DOI: https://doi.org/10.30880/ijie.2022.14.05.024
Received 26 June 2022; Accepted 15 August 2022; Available online 25 August 2022

Abstract: The application of electroplated diamond in ultrasonic vibration-assisted grinding can be a candidate to replace the manual mirror finishing of the stainless-steel surface and the ability to characterize the tool and work surfaces is important for understanding the tool-work interaction during the grinding process. In this study, an ultrasonic vibration-assisted grinding on stainless steel surface using the electroplated diamond tool is performed for the tool-work surface interaction diagnostic. The experiment used constant machining parameters, leaving the electroplated diamond tool as the only input variable. The experiment produces nine tool-work pairs for the analysis. A combination of the reversal method and areal surface metrology is introduced to capture and prepare the topography data for characterization. The analysis results show that the combination of the reversal method and areal surface metrology can be used for the electroplated diamond tool working surface characterization in explaining its effect on the ultrasonic vibration-assisted grinding of stainless-steel surface for a mirror finish.

Keywords: Surface metrology, process diagnostics, ultrasonic vibration assisted grinding, reversal method

1. Introduction

Grinding is a material removal process with undefined cutting tools. Ultrasonic vibration-assisted grinding (UVAG) is a process with ultrasonic vibration added to the tool movement besides the basic movement for the process. This study focuses on the UVAG introduced by [1] which was a 3-axis CNC milling machine equipped with an ultrasonic vibration-assisted spindle to perform face grinding using electroplated diamond tools (EDT). The application of EDT in UVAG has the potential to replace the time-consuming manual polishing for mirror-finished stainless-steel surfaces which can significantly reduce the total production time, as the grinding process can continuously be performed on the same machine after the milling process.

However, the UVAG is unstable as it requires machining parameters adjustment on every tool change [2]. Furthermore, besides the impressive grinding results, it is still unclear how the EDT abrasive working surface works to produce the mirror finish. Hence, it is necessary to analyze both surfaces, the EDT working surface, and the workpiece surface, to obtain more information related to tool-work interaction during the UVAG. The new information obtained from such a study can be used to improve the controllability of the UVAG.

*Corresponding author: mohdfauzi305@uitm.edu.my

On the other hand, the surface metrology technique may be helpful, but the standardized method is not suitable for the EDT characterization as the datum definition in surface metrology standards is an imaginary datum that is calculated based on the data obtained from the measurement and does not link to any physical datum that coincides with the machining datum [3]. Therefore, it is necessary to search for measurement and characterization techniques that coincide with the machining datum to ensure a fruitful analysis and conclusion. In traditional metrology, there is a technique called the reversal method [4] to remove measurement datum error through mechanical manipulation which changes the sign of one component of the error.

This paper introduces the combination of the reversal method and surface metrology for EDT working surface measurement to make the EDT characterization coincide with the machining datum. The analysis of ultrasonic vibration marks left by the EDT on the workpiece using Average Power Spectrum Density (PSD) to the workpiece nano-surface topography is also presented.

2. Methodology

2.1 UVAG Experimental Setup

In this study, a 3-axis CNC milling machine equipped with an ultrasonic vibration-assisted spindle system is used in the UVAG experiment. Fig. 1 shows the outline of the UVAG process for this study. The main machining conditions used are shown in Table 1. The selection of the machining condition is based on the previous study by [2] to produce a mirror finish on the stainless steel (NAK80) workpiece by combining UVAG with EDT to replace manual polishing. The rough cut of the stainless-steel workpiece is performed by the same machine prior to its cutting.

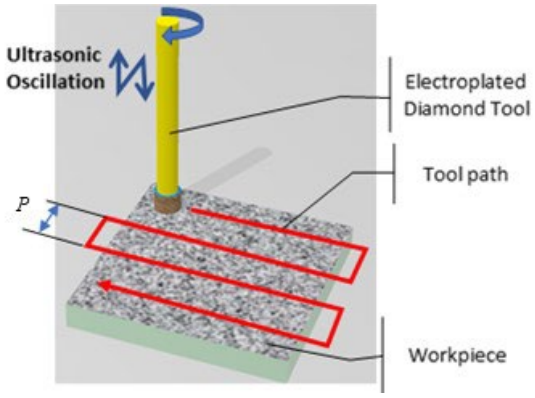

Fig. 1 - UVAG experimental process outline

Before each UVAG experiment, the EDT is set to the machine and undergoes the tool dressing or trueing process as a mirror finish is easier to be obtained with the EDT that has undergone this process [1]. The trueing process is performed using a rotated diamond truer wheel that has also been set on the same machine table. The truncation level is set into 3 levels: 1, 2, and 3 µm. The EDT working surface consists of cutting edges made by diamond grains placed on the end face of the tool substrate by nickel electroplating. The EDTs for this experiment are commercial tools with the diamond grain size #100 and grain average radius of 150 µm.

Table 1 - Machining condition for UVAG experiment

Machine	NC milling machine Makino V22	
Spindle speed	S	2000 rpm
Feed rate	F	500 mms^{-1}
Crossfeed	P	20 µm
Depth of cut	h	1 µm
Area size		6 mm × 6mm
Ultrasonic vibration	Frequency f	60 kHz
	Amplitude a	0.5 µm
Workpiece	Steel NAK80 (DAIDO steel, HRC40)	
Coolant	Oil mist (Unicut Jinen MFF)	
Tool dressing	Truncation quantities 1, 2, and 3 µm	

2.2 Reversal Method for EDT Working Surface Characterization

In surface metrology, the use of the average plane of the measured topography itself as a reference datum is a common practice. However, in this study, the EDT working surface characterization must be based on a datum that

coincides with the actual machine datum. Hence, the combination of reversal methods in surface metrology is introduced in this study.

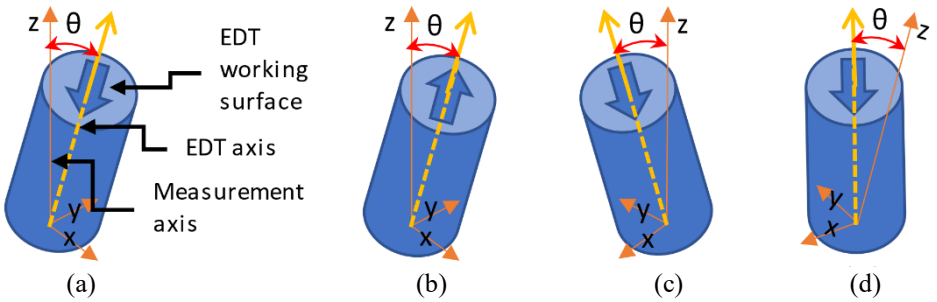

Fig. 2 - Reversal Method, (a) Initial orientation; (b) EDT is physically rotated 180° about the EDT axis; (c) Orientation (b) is digitally rotated 180°about the measurement axis; (d) Inclination is removed by (a) and (b)

In this study, the EDT is assumed to be a perfect cylinder, and the working surface is placed at one end of the cylinder. Fig. 2 depicts the reversal method designed for the EDT working surface characterization. In the initial orientation in Fig. 2(a), the EDT is fixed on the jig for the measurement for the first measurement M_1 to be captured. The first measurement M_1 consists of the surface topography F_1 and the inclination component C caused by the angle θ. The relation is as Eq. (1). The inclination component C is the measurement inclination error, a theoretically perfect plane inclined at the angle θ from the measurement XY plane, and its removal from the measurement data M_1 enables the surface topography F_1 to be levelled on a valid datum for machining functionality characterization. Hence, there is a necessity to quantify the inclination component C.

$$M_1 = F_1 + C \tag{1}$$

For the second measurement M_2, as shown in Fig. 2(b), the EDT is rotated 180° around its axis while keeping all axes' positions unchanged. As shown in Eq. (2), the measurement M_2 consists of inclination component C and the surface topography F_2, where the F_2 is congruent to the F_1 as both have the same size and shape but in the opposite direction.

$$M_2 = F_2 + C \tag{2}$$

Fig. 2(b) shows the physical analogy when measurement M_2 is digitally rotated 180° around the measurement axis while the rotation centre is assumed at the centre of the M_2 topography data. The process produces the congruent data M_2', F_2' and C' with the relation as Eq. (3).

$$M_2' = F_2' + C' \tag{3}$$

However, working surface topography F_2 is also congruent to the F_1. On the other hand, the inclination component C is a theoretical inclined plane, and rotating it 180° around the measurement axis is merely changing its sign from positive to negative. Therefore, Eq. (3) can be updated as Eq. (4).

$$M_2' = F_1 - C \tag{4}$$

The subtraction and addition process between Eq. (1) and Eq. (4) will produce the inclination component C and the surface topography F_1, accordingly (Eq. (5) and Eq. (6)). At this point, the inclination component C is a known quantity and can be removed from the measurement data M_1 (or M_2) to obtain the surface topography F_1 (or F_2). Now the F_1 is aligned on a datum that coincides with the machining axis, and the characterization result of the surface topography F_1 is expected can be correlated to the UVAG results.

$$C = \frac{M_1 - M_2'}{2} \tag{5}$$

$$F_1 = \frac{M_1 + M_2'}{2} = M_1 - C \tag{6}$$

However, when applying the actual surface topography in the reversal procedure, small misalignment and measurement noises or errors are expected, which causes unsuccessful extraction of the working surface topography F_1. The application of the cross-correlation function [9] and the least square plane [10] to the data processing, ease the implementation of the reversal method and ensure reliable results.

3. Results and Discussion

Table 2 shows the UVAG experimental data collected in this study. Each sample consists of a pair of an EDT and a workpiece. The detailed explanation of the workpiece and EDT characterization are explained in consecutive sections.

Table 2 - Experimental data

	Sample	A	B	C	D	E	F	G	H	I
UVAG process	Truncation (μm)	1	1	1	2	2	2	3	3	3
Workpiece	Areal roughness parameter (root mean square height) Sq (nm)	105.5	39.2	49.4	68.7	31.3	103.2	70.7	65.2	55.7
	σ of Sq (nm)	4.7	1.1	4.9	16. 5	3.8	2.5	14.2	3.8	3.7
	Ultrasonic marks wavelength λ_u (μm)	2	5.8	6.3	6.7	4.9	6.3	6.4	3.3	3.2
EDT	Number of Grains at top 10 μm	8	3	2	2	5	1	8	11	15
	Locus diameter of highest grain Rg (μm)	577	1620	1058	1821	1332	1800	955	914	922

3.1 Workpiece Roughness Characterization

There are two types of characterization for the workpiece surface for this study, characterization for (1) surface functionality and (2) process diagnostic.

The functional characterization of the workpiece is based on the surface roughness using the standardized areal method. The measurement using Toray Engineering SP500 White Light Interferometer (WLI) through Nikon 10× Mirau objectives which provides a 0.8 mm × 0.65 mm viewing area and 0.64 μm × 0.64 μm lateral resolution. The interferometer viewing area is used as the evaluation area for the surface topography characterization. Gaussian filtering with a cut-off wavelength λc of 0.1 mm is applied to isolate the roughness component (Ismail et al, 2014). The roughness parameter for the surface roughness quantification is the root mean square height value of the surface departures z(x, y), within the sampling area A, as in Eq. (7). The characterization result is compiled in Table 2.

$$Sq = \sqrt{\frac{1}{A}\iint_A z^2(x,y)dxdy} \tag{7}$$

3.2 Workpiece Surface Analysis for Processing Diagnostic

Based on the machining condition shown in Table 1, it is expected that the ultrasonic vibration waveform developed on the active grain locus. Eq. (8) shows the relationship between the parameters.

$$2\pi R_g = \frac{f}{s}\lambda_u \tag{8}$$

Here, R_g is the distance of the active grain from the tool rotation centre, f is the ultrasonic vibration frequency, S is the spindle rotational speed, and λ_u is the wavelength of the waveform on the finished surface which is an equivalent vertical waveform developed on the grain trajectory. It is expected that the waveform marks will have a wavelength smaller than 7 μm.

Therefore, for the process diagnostic, another set of measurements is accomplished using WLI through Nikon 50× Mirau objectives which provides a 0.18 mm × 0.133 mm viewing area and 0.131 μm lateral resolution. The measurement x-axis is manually aligned with the machining feed direction of the surface to ease the observation and analysis of the tool marks. Fig. 3(a) shows a height map of a sample workpiece nano-surface topography. The ultrasonic vibration marks are visible on the surface and the average power spectrum density (APSD) analysis indicates the existence of a constant dominant small wave with a wavelength of around 5 to 10 μm as shown in Fig. 3(b) in the tool feed direction (x-axis). These ultrasonic vibration marks are unique for each sample. Based on this phenomenon, it is suspected that there is only

one active grain that leaves the final UVAG marks on the work surface, and it must be the most protruded grain to be the one that leaves the marks. Hence, the value of ultrasonic marks wavelength λ_u is used as a parameter for further analysis and summarized in Table 2.

The above APSD analysis on the workpiece x-axis is possible because of the small size of the pick feed of 20 µm which is very small compared to the nominal tool diameter of 4 mm, hence leaving only the cutting marks that parallel with the x-axis.

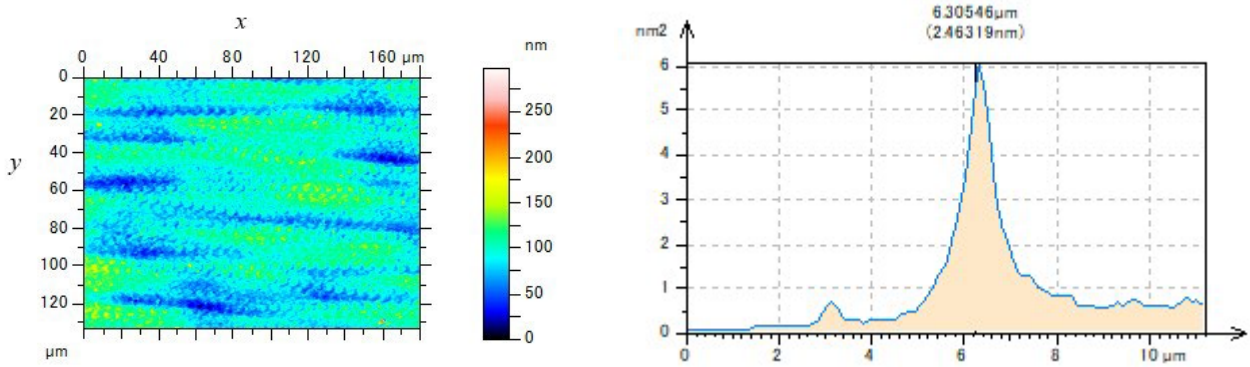

(a) (b)

Fig. 3 - Nano-surface topography data (a) and the APSD on feeding (x-axis) direction (b)

3.3 EDT working surface characterization

The measurement is accomplished using Confocal Laser Scanning Microscope LEXT OLS4000 from Olympus, through 20× objectives with a numerical aperture (N.A.) 0.6 and viewing area 640×640 µm^2, with data stitching function to combine the 4-mm diameter surface topography data from 7×7 frames. Downsampling is performed to reduce the total data points from 5448×5468 to 2022×2041 which caused the changing of the spatial data interval from 0.747×0.747 µm^2 to 2×2 µm^2, to reduce the computational burden. The outlier correction procedure [7], [8] is then applied to remove the outliers without affecting the normal data points. Two sets of surface topography data were prepared and underwent the surface reversal method.

After the reversal method, watershed segmentation is applied to the EDT surface topography to isolate each diamond grain into a feature region. Wolf pruning with 5% of S_z threshold [5], [6] is used to reduce over-segmentation. Peak's height and coordinate from each region are extracted for the EDT characterization.

The application reversal method for EDT working surface measurement enables us to coincide the characterization datum with the machining datum. Since the depth of cut of 1 µm is very small compared to the EDT surface irregularities of about 150 µm, it is suspected that there is only a small number of active grains exist, and the field parameters of surface metrology may not be useful in explaining the tool-work interaction. The application of watershed segmentation enables the identification of the active grains based on the distance of the grain's peak to the datum (reversal method). As a result, it is observed that only a small number of grains exist at the highest top 10 µm, with a minimum of one grain as in sample F. For each EDT, an active grain candidate is identified based on the highest grain, and its locus diameter R_g is estimated. The result is summarized in Table 2.

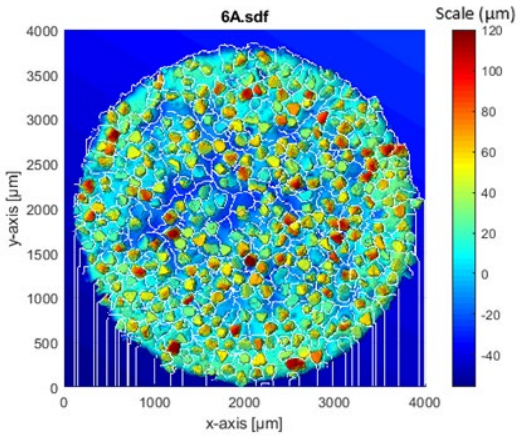

Fig. 4 - Typical EDT segmentation outcome

3.4 Comparison of Rg and PSD

Fig. 5 shows the relationship between the PSD and R_g, theoretically and experimentally. The theoretical relationship curve can be drawn by rearranging Eq. (10) as the following Eq. (9).

$$R_g = \frac{f}{2\pi S}\lambda_u \tag{9}$$

Except for the two samples, samples C and G, all experimental values are plotted about the theoretical curve, indicating that the highly protruded grain identified on the EDT using the surface reversal method is the active grain that leaves the ultrasonic vibration marks on the work surface.

However, samples C and G are located away from the theoretical line. One of the possible causes is the misalignment between the EDT's cylinder axis to the spindle rotating axis. The wobbling condition caused by the misalignment may be too small to be detected by naked eyes and may not cause problems to the machining because of its small magnitude. The misalignment can make the protruded grain on the larger locus to be in contact with the work surface despite not being the most highly protruded grain. In the case of sample C, Fig. 6 shows the identification result of the top 10 µm highly protruded grains on EDT sample C. The top 10 µm of highly protruded grains are coloured in pink and numbered from the highest to lowest of them based on the surface reversal method. As shown in the figure, there are 2 active grain candidates, grain number 3 and grain number 4, located around the locus diameter of 1700 µm which can fit the theoretical value, but they are 7 to 8 µm lower than the highest grain 1. It only requires 50 µm protruding irregularities on the EDT cylinder surface to produce the angular error of 2 degrees and make the grain at the larger locus diameter, grains 3 and 4, be the active grain that leaves the ultrasonic marks on the work surface during the UVAG. Another possible reason is the irregularities in the EDT cylindricity, which is also the physical reference of the measurement and can easily affect the accuracy of the surface reversal method.

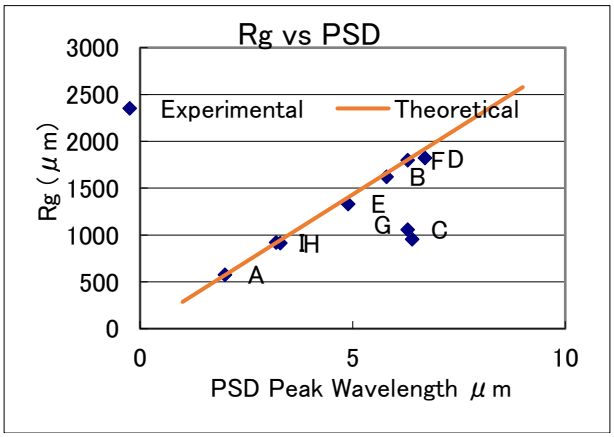

Fig. 5 - Relationship of R_g and PSD

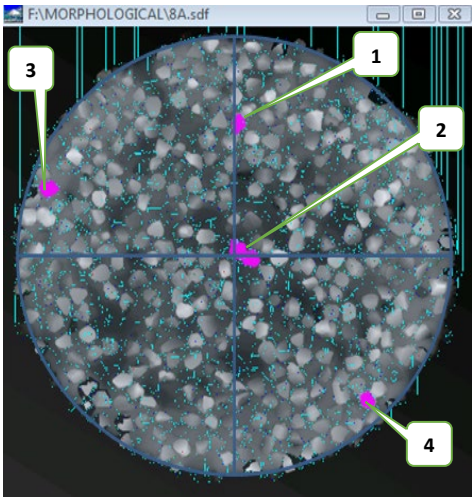

Fig. 6 - Top 10 micrometre highly protruded grains on EDT sample C

From this analysis, there is an active grain that caused the ultrasonic vibration marks on the grain and the locus diameter R_g can be derived from the surface topography analysis of the workpiece. Hence, in the next analysis, the value of active grain locus diameter R_g is based on the derivation from ultrasonic vibration marks wavelength λ_u, as a parameter to represent the EDT.

3.5 Comparison of R_g and S_q

Fig. 7 shows the relationship between EDT active grain locus diameter R_g and workpiece surface roughness parameter S_q. A polynomial trendline is inserted in the plot with a correlation coefficient R^2 of 0.6, which indicates a certain level of a nonlinear relationship between the two parameters. This graph also indicates that there is an optimum value of R_g at around 1300 µm for the smallest roughness S_q.

This phenomenon is probably due to the active grain locus pattern developed on the surface, as different active grain locus diameters R_g create different locus patterns on the workpiece, especially at the area of the crossfeed P between the tool paths. For the given machining condition, the locus pattern curves at this area are evenly distributed when the locus diameter R_g is around 1350 µm, hence producing the lowest roughness parameter S_q. The gap between the locus line becomes bigger when the R_g is lower than 1350 µm, and the distribution of the locus lines and the gaps become uneven when the R_g is higher than 1350 µm, in either case causing higher roughness parameter R_g. This is a similar phenomenon as simulated and demonstrated in the lathe by [11] where the distance between cutting tool traces affects the roughness of the turned surface. The different R_g between EDTs is also the reason for the need to change the machining parameter for every tool change in the actual application of the UVAG, as the best cutting tool traces arrangement can be obtained by machining parameters adjustment for any given R_g.

Even though this study indicates the existence of one active grain of each EDT that leaves the final ultrasonic vibration marks and their influences on the work roughness S_q, it cannot deny the contribution of multi-active grains in the UVAG. However, we can say that there is a very small number of active grains that contribute to the UVAG for the given machining condition. Additionally, developing the EDT with the known R_g may be useful to improve the controllability of the UVAG.

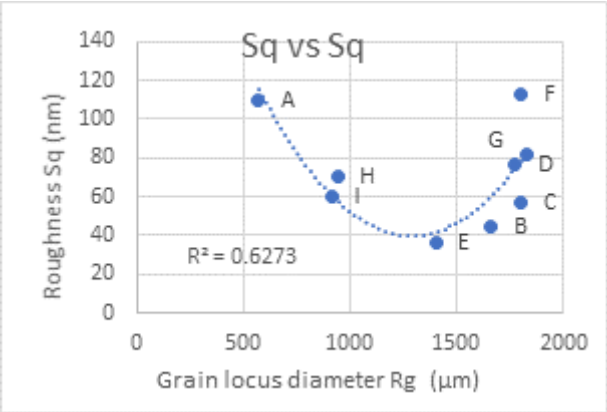

Fig. 7 - Roughness and active grain locus diameter

4. Conclusions

The conclusion of this study is as follows.

- The reversal method introduced is useful to characterize the EDT and find the active grain candidates.
- There is only a small amount of diamond grains that are active and contribute to the surface finishing during the UVAG. There is likely only one grain that leaves the final ultrasonic vibration marks and influences the final roughness of the workpiece.
- There is an optimum location of the active grains on the EDT working surface for the given UVAG process parameters.
- The analysis of the nano-topography of the workpiece is useful for the UVAG diagnostic and confirmed the reversal method based on active grain identification.
- The information gained from this study can be used to design EDT that can increase the controllability of the UVAG process.

Acknowledgement

The authors acknowledge the Ministry of Higher Education (MOHE) Malaysia for the financial support given under the Fundamental Research Grant Scheme (FRGS) with a Grant No: FRGS/1/2018/TK03/UiTM/02/03. The authors acknowledge the College of Engineering, University Teknologi MARA for the research and publication opportunities.

References

[1] Hara K., Isobe H., Kyusojin A., & Okada M., (2008) Study on mirror surface grinding of die steel by using ultrasonically assisted diamond tools, International Journal of Abrasive Technology 1(3/4):265 - 273
[2] Hara, K., Isobe, H., Ismail, M. F., & Kaihotsu, S. I. (2011). Effects of cutting edge truncation on ultrasonically assisted grinding. Advanced Materials Research, 325, 97–102.
[3] Ismail, M. F., Yanagi, K., & Isobe, H. (2011). Characterization of geometrical properties of electroplated diamond tools and estimation of its grinding performance. Wear, 271(3–4), 559–564.
[4] Evan, C. J., Hocken, R. J., & Estler, W. T. (1996). Self-calibration: Reversal, redundancy, error separation, and "absolute testing". Annals of the CIRP, 45(2), 617–634.
[5] Ismail, M. F., Zaini, N. H., Jaafar, T. R., & Che Pin, N. (2015). Demonstration of watershed segmentation on simulated surface topography data. Jurnal Teknologi, 10, 49–52.
[6] Lou, S., Pagani, L., Zeng, W., Jiang, X., & Scott, P. J. (2020) Watershed segmentation of topographical features on freeform surfaces and its application to additively manufactured surfaces. Precision Engineering, 63(February), 177–186.
[7] Ismail, M.F., Yanagi, K., & Fujii, A. (2010). An outlier correction procedure and its application to areal surface data measured by optical instruments. Measurement Science and Technology, 21(10), 105105.
[8] Ismail, M. F., Jaafar, T. R., Che Mat, S., & Pahmi, M. A. A. H. (2014). Evaluation of outlier-specific correction procedure for areal surface texture. Applied Mechanics and Materials, 661, 137–142.
[9] Buck, John R., Michael M. Daniel, and Andrew C. Singer. (2002) Computer explorations in signals and systems using MATLAB®. Prentice-Hall.
[10] Rao, C. R., & Toutenburg, H. (1995). Linear models: Least squares and alternatives. Springer-Verlag.
[11] Xie, D., & Wang, M. (2012). Study on surface roughness simulation to lathe machining. Advanced Materials Research, 538-541, 1373-1376.